CrossMark

ORIGINAL PAPER

Evaluation of CMIP5 models for projection of future precipitation change in Bornean tropical rainforests

Mubasher Hussain[1,2,3] · Khamaruzaman Wan Yusof[2] ·
Muhammad Raza Ul Mustafa[2] · Rashid Mahmood[4] · Shaofeng Jia[4]

Abstract We present the climate change impact on the annual and seasonal precipitation over Rajang River Basin (RRB) in Sarawak by employing a set of models from Coupled Model Intercomparison Project Phase 5 (CMIP5). Based on the capability to simulate the historical precipitation, we selected the three most suitable GCMs (i.e. ACCESS1.0, ACCESS1.3, and GFDL-ESM2M) and their mean ensemble (B3MMM) was used to project the future precipitation over the RRB. Historical (1976–2005) and future (2011–2100) precipitation ensembles of B3MMM were used to perturb the stochastically generated future precipitation over 25 rainfall stations in the river basin. The B3MMM exhibited a significant increase in precipitation during 2080s, up to 12 and 8% increase in annual precipitation over upper and lower RRB, respectively, under RCP8.5, and up to 7% increase in annual precipitation under RCP4.5. On the seasonal scale, Mann-Kendal trend test estimated statistically significant positive trend in the future precipitation during all seasons; except September to November when we only noted significant positive trend for the lower RRB under RCP4.5. Overall, at the end of the twenty-first century, an increase in annual precipitation is noteworthy in the whole RRB, with 7 and 10% increase in annual precipitation under the RCP4.5 and the RCP8.5, respectively.

1 Introduction

From 1951 to 2010, emission of greenhouse gases (GHG) has caused a global surface warming ranging from 0.5 to 1.3 °C (IPCC 2013). Continued emission of GHG will trigger further atmospheric warming to change the equilibrium of the global climate system. Climate change impact on various climate variables, such as precipitation and temperature, is being assessed by employing general circulation models (GCMs). Recently, a new generation of GCMs has become available from Coupled Model Intercomparison Project Phase 5 (CMIP5); these GCMs are being evaluated over the various regions for climate change's impact assessment. The CMIP5 models provide a new avenue for modelling climate change impact by employing four alternative scenarios called representative concentration pathways (RCPs) (Venkataraman et al. 2016). Representing model physics, spatial resolution, and the inclusion of atmospheric aerosols; the CMIP5 models are better compared to the Coupled Model Intercomparison Project Phase 3 (CMIP3) models (Sperber et al. 2012; Taylor et al. 2012); particularly for Asian-Australian monsoon circulation, the CMIP5 models have been renowned better than the CMIP3 (Wang et al. 2013).

Several GCMs from CMIP5 are being recommended for various regions; however, using a single GCM for future precipitation projection over a river basin would result in misleading the climate change assessment (Tan et al. 2015).

✉ Mubasher Hussain
MubasherHussain@sarawakenergy.com.my;
mubasherghumman@gmail.com

1 Hydro Department, Sarawak Energy Berhad,
93050 Kuching, Sarawak, Malaysia

2 Department of Civil and Environmental Engineering, Universiti Teknologi Petronas, 32610 Seri Iskandar, Perak, Malaysia

3 Bintech Limited, Folkestone CT20 2PT, Kent, England

4 Key Laboratory of Water Cycle and Related Land Surface Processes / Institute of Geographic Science and Natural Resources Research, Chinese Academy of Sciences, Beijing 100101, China

⚙ Springer

Therefore, evaluation of a set of CMIP5 models is essential to explore the suitability of each model for simulating present-day precipitation and further application for future precipitation projection over a river basin. Recently, few studies, i.e. McSweeney et al. (2015), Sharmila et al. (2015), and Siew et al. (2013), have conducted the evaluation of CMIP5 models over South Asia and South East Asia (SEA) as described in Table 1. Each of these studies recommended a couple of GCMs for climate change's impact assessment for these regions.

Tropical rainforests are generally located at latitudes within 10° north and south of the equator. Dominated by the intertropical convergence zone (ITCZ), the climate of tropical rainforests is typically hot and wet throughout the year. These regions do not have the summer or winter, and precipitation in the form of rainfall is heavy and frequent throughout the year. The tropical rainforests are the most commonly found in SEA, Central Africa, and South America. The Rajang River Basin (RRB) of Sarawak covers major tropical rainforests of the SEA. In the context of the climate change impact on future precipitation, Sarawak attracted little attention in the past researches. Kumagai et al. (2004) projected precipitation over Lambir Hills National Park in Sarawak using HadCM3 and found drier DJF, little change in MAM, wetter JJA, and SON during 2080s compared to the baseline period of 1968–2001. Amin et al. (2016) assessed the climate change impact on water resources in Sarawak and Sabah using two GCMs from the CMIP3 and revealed that climate change would have uneven effect over this region due to complex and steep regional topography. Loh et al. (2016) simulated future precipitation over Malaysia for 2071–2099 using PRECIS modelling system and found that HadCM3Q0/PRECIS produces slightly wetter condition compared with the APHRODITE data (1966–1990) especially over central Borneo and northeastern Peninsular Malaysia. Hussain et al. (2017a) assessed the climate change resilience of Batang Ai reservoir in western Sarawak using five GCMs from CMIP5 and revealed the seasonal shift of precipitation over the study area. Another recent study by (Hussain et al. 2017b) projected the future changes in precipitation at three stations in Sarawak, i.e. Kuching, Bintulu, and Limbang; they also noted a seasonal shift in future precipitation with decrease

Table 1 Summary of recent studies conducted for evaluation of CMIP5 models over South and South East Asian region

Study	Evaluation variable	No. of CMIP5 models evaluated	Study area	Recommended models	Key results
(Siew et al. 2013)	Winter monsoon	10	SEA	CNRM-CM5 IPSL-CM5A-MR NorESM1-M	All GCMs simulated the spatial pattern of winter monsoon rainfall but with a large spread of wet bias magnitude over the SEA. Three most skilful models based on simulating present day winter monsoon over SEA are selected for future projection.
(McSweeney et al. 2015)	Precipitation and temperature	40	SEA	HadGEM2-ES ACCESS1-0 ACCESS1-3 BCC-CSM1-1-m BNU-ESM CanESM2 CMCC-CM CCSM4 CNRM-CM5 GFDL-CM3 GFDL-ESM2G GFDL-ESM2M IPSL-CM5A-MR MPI-ESM-MR	14 out of 40 models are declared as the satisfactory for future projection of precipitation and temperature over SEA.
(Sharmila et al. 2015)	Summer monsoon	20	Indian sub-continent	BNU-ESM MIROC5 MPI–ESM–LR NorESM1–M	Out of 20 GCMs, four models reproduced Indian summer monsoon variability.
This study	Precipitation	20	Central Sarawak (Borneo Island)	ACCESS1.0 ACCESS1.3 GFDL-ESM2M	Most out of 20 models were unable to simulate intra-annual variability in term of monthly precipitation. Three selected models followed the variation of observed monthly precipitation over the Central Sarawak and their mean ensemble is used for future precipitation projection over RRB.

in precipitation during December to February and increase in precipitation during the June to August.

Numerous studies have developed climate change scenarios for precipitation projection in various Asian regions using different downscaling techniques for transforming observed climate data into likely future scenarios (Chu et al. 2010; Hasan et al. 2017; Hassan et al. 2014; Hasson et al. 2016; Juneng et al. 2016; Loh et al. 2016; Mahmood and Babel 2012). Weather generators (WGs) are being used to generate multiple years' climate change scenarios on the daily time scale, i.e. Forsythe et al. (2014), Jones et al. (2011), Kilsby et al. (2007), Semenov and Barrow (2002), Semenov and Barrow (1997), Semenov et al. (1998), and Wilks (2010). Several WGs have been developed for generation of time series for climate variable, i.e. WGEN (Richardson 1981; Richardson and Wright 1984), USCLIMATE (Hanson et al. 1994), CLIGEN (Nicks et al. 1995), ClimGen (Stockle et al. 1999), and LARS-WG (Semenov and Barrow 2002). These WGs perform well for preserving the total amount of precipitation; however, most of them underestimate the monthly and interannual variance of precipitation (Buishand 1978; Chen et al. 2009; Gregory et al. 1993; Hansen and Mavromatis 2001; Johnson et al. 1996; Katz and Parlange 1993; Wilks 1989; Wilks 1999; Zhang and Garbrecht 2003).

Chen et al. (2010) developed a WG known as WeaGETS addressing the low frequency variability (LFV) in generated precipitation and temperature. It has been evaluated for precipitation generation in sub-arctic climate of Canada (i.e. Chen et al. 2010) and semi-arid climate of China (i.e. Chen and Brissette 2014); where it successfully generated the variability in monthly, seasonal, and annual precipitation. However, WeaGETS has not been evaluated yet for precipitation generation over tropical regions, i.e. tropical rainforest in SEA where the issue of LFV in monthly and seasonal precipitation is of high concern. Therefore, this study assessed the capability of WeaGETS for generating precipitation over the Bornean tropical rainforests, i.e. RRB in Sarawak.

Recently, ensemble techniques such as change factor approaches have also received increased attention for climate change's impact assessment, i.e. Fowler and Ekström (2009), Knutti et al. (2010), Ntegeka et al. (2014), and Teutschbein and Seibert (2010). Due to high uncertainties involved with climate model parameters, ensemble techniques are being preferred (Collins 2007). However, traditional change factor approach in ensemble technique only changes the mean value and disregards several statistical factors such as frequency, temporal sequencing, and variability. Therefore, alternative approaches such as quantile scaling, mapping, and perturbation have been proposed (Chiew et al. 2009; Ntegeka et al. 2014; Olsson et al. 2009). These techniques perturb precipitation intensities with percentile-based factor calculated from the control and future precipitation ensembles. These approaches are also suitable for the regions receiving increased variability in precipitation events (Ntegeka et al. 2014), i.e. tropical rainforests where heavy precipitation events increase at higher rates compared to mild events.

In this study, we evaluated 20 GCMs from CMIP5 for their capability to simulate historical precipitation over the RRB and presented projected changes in future precipitation over the RRB. Therefore, the objectives of this study were the following: (i) to evaluate the fidelity of 20 GCMs in simulating the monthly precipitation variability over the RRB under present day climate (1976–2005), (ii) performance evaluation of WeaGETS for simulating monthly precipitation over the RRB, and (iii) to investigate the potential change in future precipitation over the RRB illuminating the emerging role of increased GHG emission for changing precipitation over the Bornean tropical rainforests.

## 2 Study area and data description

2.1 Study area

The RRB is the largest river basin in the Sarawak state of Malaysia located on the Borneo Island (Fig. 1)—which is the largest island in Asia and third largest island in the world. The RRB has the total catchment area of about 50,000 km^2 and covers 40% of the Sarawak's tropical rainforests. The precipitation in the form of rainfall is abundant in the RRB with average annual rainfall ranging from 3000 to 5200 mm over the river basin. The catchment elevations vary from sea level at the west coast to 2016 m above sea level in the upper part of the RRB. Rajang River is also the longest river in Malaysia; with a total length of 563 km, it is also the largest source of fresh water in Malaysia. The Rajang River originates from the Iran Mountains, a range of mountains on the border between Malaysia and Indonesia, and drains to the South China Sea.

The region has two monsoon seasons, the northeast monsoon (October to March) and the southwest monsoon (May to September); the northeast monsoon brings more precipitation in the RRB compared to the southwest monsoon. The months of December to February are considered the wettest months of the year and June to August are the lowest precipitation months. In this study, annual precipitation cycle was divided into four quarters—December to February (DJF), March to May (MAM), June to August (JJA), and September to November (SON).

2.2 Data used

2.2.1 Historical precipitation data

Historical daily precipitation for 36 rainfall stations (as shown in Fig. 1) was obtained from the Department of Irrigation and
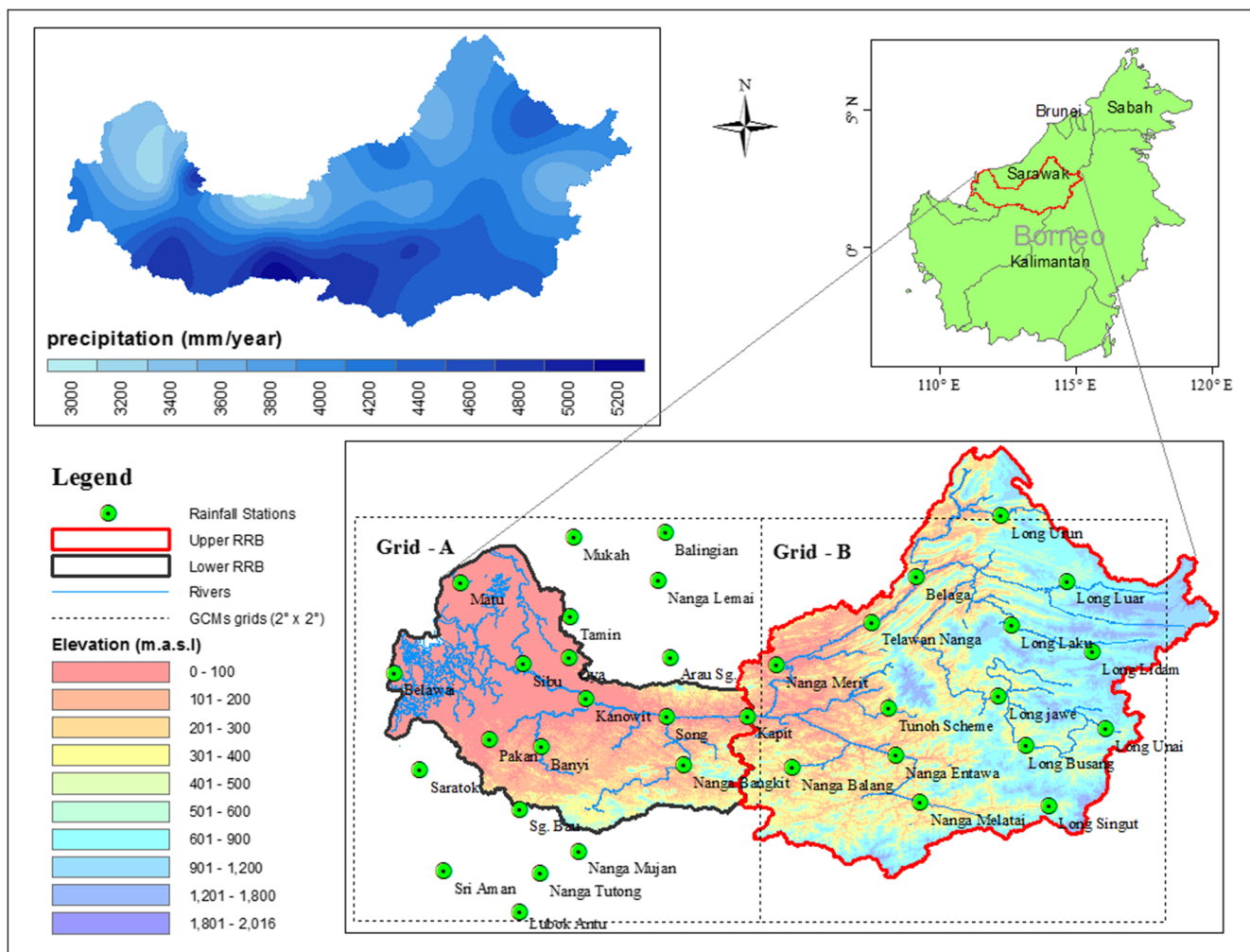
Fig. 1 Location of RRB in Borneo Island, selected rainfall stations, rivers network, elevations, and historical average annual precipitation in RRB

Drainage, Sarawak for a period of 1976–2005. Out of these rainfall stations, 25 stations are located in the RRB and 11 stations in the neighbour river basins.

2.2.2 CMIP5 models and experiment

During evaluation of GCMs, daily precipitation ensembles of 20 GCMs from CMIP5 (as listed in Table 2) were used for their historical simulations (1976–2005). The historical simulations are based on the observed climate forcing; initial conditions of historical simulations are based on fixed pre-industrial forcing (Sharmila et al. 2015). The SEA is one of the most vulnerable regions to the climate change and it has already witnessed the increased intensity of storms such as Typhoon Haiyan in the Philippines during November 2013. Raitzer et al. (2015) stated that five of the Southeast Asian countries, i.e. Indonesia, Malaysia, the Philippines, Thailand, and Vietnam, contribute 90% of the regional GHG emission and would face significant reduction in their GDP by 2100. Indonesia and Malaysia have the largest land use area covered

with forest and continued deforestation in these two countries contributes to the most of the regional GHG emission; therefore, the region is one of the most vulnerable regions to climate changes. The RCP4.5 is a moderate climate scenario in which the total radiative forcing will be stabilised to 4.5 Wm^{-2} in the year 2100. The RCP 8.5 (strongest scenario) runs are forced with relatively high anthropogenic GHG emissions; under RCP8.5, the radiative forcing will increase and then stabilise at about 8.5 Wm^{-2} after 2100. Initial conditions for the RCP4.5 and the RCP8.5 start from the end of the historical runs. Two of the selected models during the evaluation (i.e. ACCESS10 and ACCESS13) only provide the future projection under RCP4.5 and RCP8.5. Therefore, to assess the future changes in precipitation, we presented the RCP4.5 and RCP8.5 projection over the RRB. The ensemble member (r1i1p1) for future run (2011–2100) of each selected model run was used in this study; same ensemble member was adopted by Kitoh et al. (2013) and Sharmila et al. (2015). The historical and future precipitation ensembles were downloaded from the IPCC Data Distribution Center (IPCC-

DDC) website (http://www.ipcc-data.org/sim/gcm_monthly/AR5/Reference-Archive.html) in the netCDF data format for the whole globe (latitude 90° N to 90° S and longitude 180° W to 180° E).

3 Methodology

3.1 Evaluation of CMIP5 models

All of the 20 selected GCMs have different spatial resolutions varies between (1.12° × 1.12°) and (2.8° × 2.8°) as shown in Table 2. Therefore, all GCMs were regridded into the same grid size of (2.0° × 2.0°) through bilinear interpolation to minimise the effect of spatial resolution on our comparison. The main reasons for regridding all GCMs at (2.0° × 2.0°) are to bring the grids to the average grid size of the selected GCMs and to provide opportunity to use maximum rainfall stations in the grid for evaluation. The Grid Analysis and Display System (GrADS) developed by Doty (1995) was utilised to re-grid all 20 GCMs.

The study area lies in the two grids, i.e. Grid-A and Grid-B as shown in Fig. 1. Grid-A covers the high altitudes, mid-land, and coastal areas, whereas Grid-B mostly covers the higher altitudes only. Grid-A also has the continuous record of precipitation data without any longer missing period and also has higher density of rainfall stations (i.e. 21 rainfall stations) compared to Grid-B. Therefore, Grid-A was selected for GCM evaluation during their historical run. The observed monthly precipitation at all rainfall stations in the Grid-A was averaged over the grid using the Thiessen polygons method. In terms of their precipitation mechanism, all of the stations in Grid-A have the same precipitation pattern as shown in Fig. 2, where DJF are the wettest months and JJA are the driest months compared to the rest.

All of the precipitation ensembles from the 20 GCMs were evaluated with the observed precipitation using the following statistical indicators—correlation coefficient (R), normalised standard deviation (NSD), root mean square error (RMSE), and mean absolute error (MAE). The optimistic evaluation criteria of greater value of R and NSD closer to unity are designed by Taylor (2001) and being used by various recent studies, i.e. Hassan et al. (2015), Sarthi et al. (2015), and Sharmila et al. (2015). In addition to these two statistical

Table 2 Basic information of CMIP5 models selected for evaluation over the study area

Modelling center acronym	Modelling center expansion	Model name	Horizontal resolution (lon × lat)	Identifier
CSIRO-BOM	Commonwealth Scientific and Industrial Research Organization (CSIRO) and Bureau of Meteorology, (BOM), Australia	ACCESS1.0	1.875° × 1.25°	1
		ACCESS1.3	1.875° × 1.25°	2
BCC	Beijing Climate Centre, China Meteorological Administration, China	BCC-CSM1.1	2.8° × 2.8°	3
		BCC-CSM1.1 m	2.8° × 2.8°	4
BNU	College of Global Change and Earth System Science, Beijing Normal University, China	BNU-ESM	2.8° × 2.8°	5
CCCma	Canadian Centre for Climate Modelling and Analysis, Canada	CanESM2	2.8° × 2.8°	6
CSIRO-QCCCE	Commonwealth Scientific and Industrial Research Organization in collaboration with the Queensland Climate Change Centre of Excellence, Australia	CSIRO-Mk3.6.0	1.875° × 1.865°	7
NOAA-GFDL	Geophysical Fluid Dynamics Laboratory, USA	GFDL-CM3	2.5° × 2.0°	8
		GFDL-ESM2G	2.0° × 2.0°	9
		GFDL-ESM2M	2.5° × 2.0°	10
NIMR, KMA	National Institute of Meteorological Research, Korea Meteorological Administration, South Korea	HadGEM2-AO	1.875° × 1.25°	11
MOHC	Met Office Hadley Centre, UK	HadGEM2-ES	1.875° × 1.25°	12
INM	Institute for Numerical Mathematics, Russia	INMCM4	2.0° × 1.5°	13
IPSL	Institut Pierre-Simon Laplace, France	IPSL-CM5A-MR	2.5° × 1.267°	14
MIROC	Atmosphere and Ocean Research Institute (The University of Tokyo), National Institute for Environmental Studies, and Japan Agency for Marine-Earth Science and Technology, Japan	MIROC5	1.4° × 1.4°	15
		MIROC-ESM-CHEM	2.8° × 2.8°	16
MPI-M	Max Planck Institute for Meteorology (MPI-M), Germany	MPI-ESM-LR	1.875° × 1.865°	17
		MPI-ESM-MR	1.875° × 1.865°	18
MRI	Meteorological Research Institute, Japan	MRI-CGCM3	1.12° × 1.12°	19
NCC, NMI	Norwegian Climate Centre, Norway	NorESM1-M	2.5° × 1.9°	20
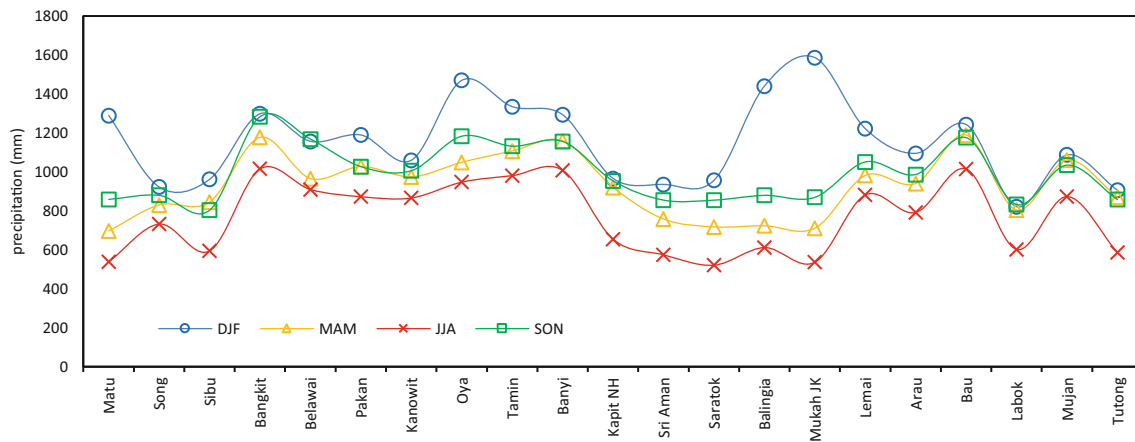
Fig. 2 Seasonal precipitation (1976–2005) over 21 rainfall stations in Grid-A

indicators, we also analysed the RMSE and MAE to assess the capability of all GCMs for simulating monthly precipitation over the study area. We defined the criteria to select the highest ranked models for the study area as shown in Table 3.

3.2 Precipitation generation using WeaGETS

In this study, WeaGETS was used to simulate the future precipitation at the 25 rainfall stations in the RRB. WeaGETS is a Matlab based stochastic WG; it has the options to employ the first-, second-, and third-order Markov chain model for the precipitation occurrence and gamma and exponential distribution for generation of precipitation amount during the wet days. Several studies concluded that higher-order Markov chain models provide in-depth insights of precipitation phenomenon compared to the first-order Markov chain, i.e. Chen and Brissette (2014), Islam and Chowdhury (2006), Stephenson et al. (1999), and Veldkamp et al. (2016). The gamma distribution has been successfully used to model the distribution of wet-day precipitation amounts in several studies such as Chen et al. (2010), Groisman et al. (2005), Semenov and Bengtsson (2002), Watterson and Dix (2003), and Wilby and Wigley (2002). Therefore, third-order Markov chain model was adopted for the simulation of precipitation occurrence and gamma distribution for the generation of precipitation amount at all rainfall stations in the RRB.

LFV in generated daily precipitation was corrected at the monthly and annual scales taking into account the power spectra of observed precipitation at the same scale. The power spectra were computed by fast Fourier transformation; the detailed methodology for the LFV correction in WeaGETS is described in Chen et al. (2010). Time series data for observed precipitation (1976–2005) at all 25 rainfall stations was used in the WeaGETS to generate the 120-year precipitation time series. The performance of model for generating the future precipitation was assessed using three statistical indicators, i.e. Nash–Sutcliffe model efficiency (NSE), mass balance error (MBE), and

RMSE. The NSE is a normalised statistic that provides the relative degree of the residual variance compared to the observed variance (Nash and Sutcliffe 1970), and it is calculated as:

$$NSE = 1 - \frac{\sum_{i=1}^{n} \left(P_{\text{obs,i}} - P_{\text{gen,i}} \right)^2}{\sum_{i=1}^{n} \left(P_{\text{obs,i}} - \overline{P_{\text{obs}}} \right)^2} \tag{1}$$

where $P_{\text{obs, i}}$ is the ith observed precipitation, $P_{\text{gen, i}}$ is the ith generated precipitation, $\overline{P_{\text{obs}}}$ is the mean of the observed precipitation, and n is the total number of observations. The value of NSE equal to 1 indicates the perfect match between the observed and generated precipitation.

The MBE is another performance indicator for the generated precipitation; it shows capability of the model to generate the total amount of precipitation and is calculated as:

$$MBE = \frac{\sum_{i=1}^{n} P_{\text{gen,i}} - \sum_{i=1}^{n} P_{\text{obs,i}}}{\sum_{i=1}^{n} P_{\text{obs,i}}} \tag{2}$$

The MBE of zero indicates the perfect agreement between the observed and generated precipitation.

The RMSE is also one of the frequently used statistical error index for generated and observed data (Campozano et al. 2016; Kum et al. 2014; Mahmood and Babel 2012) and is calculated as:

$$RMSE = \sqrt{\frac{\sum_{i=1}^{n} \left(P_{\text{obs,i}} - P_{\text{gen,i}} \right)^2}{n}} \tag{3}$$

RMSE of zero indicates the perfect agreement between the observed and generated precipitation.

3.3 Quantile-based precipitation perturbation under future scenarios

To explore the climate change impact on precipitation variability over the RRB, stochastically generated precipitation at

Table 3 Performance of CMIP5 models over the Grid-A; selected models are as highlighted

CMIP5 Model	R R > 0.4	NSD 0.7 > NSD > 1.3	RMSE RMSE < 135	MAE MAE < 70	Rank (out of 4)
ACCESS1.0	**0.45**	**1.24**	**116**	**43**	4
ACCESS1.3	**0.41**	**1.29**	**133**	**61**	4
BCC-CSM1.1	0.07	1.79	184	**41**	1
BCC-CSM1.1m	0.25	**1.12**	188	147	1
BNU-ESM	0.08	**0.85**	142	86	1
CanESM2	0.29	**0.73**	173	145	1
CSIRO-MK3.6.0	0.14	1.78	175	**34**	1
GFDL-CM3	0.21	1.56	167	74	0
GFDL-ESM2G	0.16	1.74	168	**14**	1
GFDL-ESM2M	**0.54**	**1.27**	**127**	**67**	4
HadGem2-AO	0.36	1.48	140	**69**	1
HadGem2-ES	0.20	**0.79**	155	116	1
INMCM4	-0.01	**0.81**	156	105	1
IPSL-CM5A-MR	0.02	1.92	196	**33**	1
MIROC-ESM-CHEM	0.02	0.46	**120**	**69**	2
MIROC5	-0.01	**0.98**	152	84	1
MPI-ESM-LR	-0.26	**1.09**	181	102	1
MPI-ESM-MR	-0.18	**1.26**	190	107	1
MRI-CGCM3	0.19	1.64	164	**47**	1
NorESM1-M	0.30	**1.20**	158	105	1

all stations was perturbed by quantile-based perturbation approach. For this purpose, we used the control run (1976–2005) and future runs (2011–2100) of best three models' mean ensemble (B3MMM) to derive the quantiles factors. The reason to perturb the stochastically generated future precipitation time series is to minimise the biases which would be introduced by WG if we perturb the observed precipitation prior to use in WG. Using a synthetic time series of precipitation for perturbation also provides an additional opportunity to explore the interannual and seasonal variability compared to the simply perturbing the historical 30-year observed time series (Forsythe et al. 2014).

The generated time series at each rainfall station for the period of 2011–2040 (2020s), 2041–2070 (2050s), and 2071–2100 (2080s) were separately perturbed in two steps. In the first step, wet-day frequency perturbation was applied to 30-year time series and then perturbation for wet-day intensity quantile was done. Wet-day frequency perturbation was calculated from the B3MMM ensemble as the ratio of the number of wet days in a given month during the future scenario period (i.e. 2080's) to the number of wet days during the corresponding month in the control period (1976–2005). This calculated perturbation was applied to the stochastically generated future precipitation time series at all stations for the

same future period (i.e. 2080's) as used for the B3MMM. In the second step, the wet-day quantile perturbation was calculated based on wet-day quantiles in the control period (1976–2005) of the B3MMM to the wet-day quantiles in the scenario period (i.e. 2080's) of the B3MMM. As the number of wet days varies in the control and scenario period, therefore, the wet-day intensity perturbation was calculated as the ratio of control and scenario quantiles having same exceedance probability. Then, this perturbation was applied to the same quantiles in the stochastically generated future precipitation for the same period (i.e. 2080s). The precipitation perturbation process adopted in this study is the same as used by Ntegeka et al. (2014).

3.4 Trend analysis

Trend analysis is commonly used for the climate change impact studies, i.e. Chattopadhyay and Edwards (2016), Groisman et al. (2005), and Timbal (2004). Recently, Mann-Kendall's trend test is being used for the precipitation trend analysis such as Chattopadhyay and Edwards (2016) and Feng et al. (2016). To identify the significance in the data at stations having large magnitude of the changes, the Mann Kendall (MK) trend test is the most appropriate statistical analysis (Hirsch et al. 1982). The purpose of the MK test is

to assess the monotonic trend upward (downward) of a variable over a time; it illustrates that the variable increases or decreases consistently through the time (Gilbert 1987; Kendall 1975; Mann 1945). MK test assumes that there is no trend in data as the null hypothesis (H_0) and it is tested against the alternate hypothesis (H_1), which assumes that there is a trend. For a precipitation time series of n values where P is the precipitation at time T, assuming a pair (P_i, T_i and P_j, T_j) where $1 \leq I \leq j \leq n$. If the $P_i - P_j$ and $T_i - T_j$ have the same sign, then it is called concordant pair; otherwise, it is called discordant pair and if the difference is zero, then the pair is called tied. The Kendall's τ is calculated as:

$$Kendall's\ \tau = \frac{n_c - n_d}{\sqrt{[n(n-1)/2 - \sum t_i(t_i-1)/2] \times [n(n-1)/2 - \sum u_i(u_i-1)/2]}}$$
(4)

where n_c is the number of concordant pair and and n_d is the number of discordant pairs; t_i is the number of tied value for a specific rank of precipitation and u_i is the number of tied values for time period.

We performed the Mann-Kendall trend test to estimate the trend in annual and seasonal precipitation in the RRB for the historical period of 1976–2005 and future period of 2011–2100 under both RCPs. The results are discussed in Sect. 4.4.

4 Results and discussion

4.1 Evaluation of GCMs

Using the defined criteria described in Sect. 3.1, three models with highest rank were selected as the most suitable models for future precipitation projection over the RRB. Among all 20 GCMs, ACCESS1.0, ACCESS13, and GFDL-ESM2M were ranked highest during the evaluation process. Most of the models were unable to simulate monthly precipitation during control run of 1976–2005; Fig. 3 shows the time series plot of the monthly precipitation simulated by all GCMs compared with the monthly observed precipitation over the Grid-A. On the other hand, the selected three models followed the variation of observed precipitation reasonably. The B3MMM was also compared with the observed monthly precipitation (Fig. 3) and it followed the pattern of observed precipitation well; Therefore, B3MMM was selected to explore future changes in precipitation over the RRB. The other two models HadGem2-AO and NorESM1-M have the higher correlation compared to the rest of unselected GCMs but did not performed well for the other statistical indicators (Table 3) and therefore not considered for the future precipitation projection over the RRB.

McSweeney et al. (2015) conducted an evaluation of CMIP5 models over the SEA; out of 40 GCMs, 14 GCMs were declared satisfactory for their capability to simulate the observed climate of SEA (as listed in Table 1). After the screening, McSweeney et al. (2015) tested the selected 14 GCMs for their performance over the Singapore and noted that four out of 14 shortlisted GCMs were unable to reproduce the observed climate over the Singapore; therefore, they selected ten GCMs for future projection of precipitation and temperature over the Singapore. In this study, the three highest ranked models, i.e. ACCESS1.0, ACCESS1.3 and GFDL-ESM2M, are among the 14 models selected by McSweeney et al. (2015). However, most of the other models that performed satisfactory overall for the SEA (McSweeney et al. 2015) do not reproduce observed precipitation realistically over the Central Sarawak. Therefore, ACCESS1.0, ACCESS1.3, and
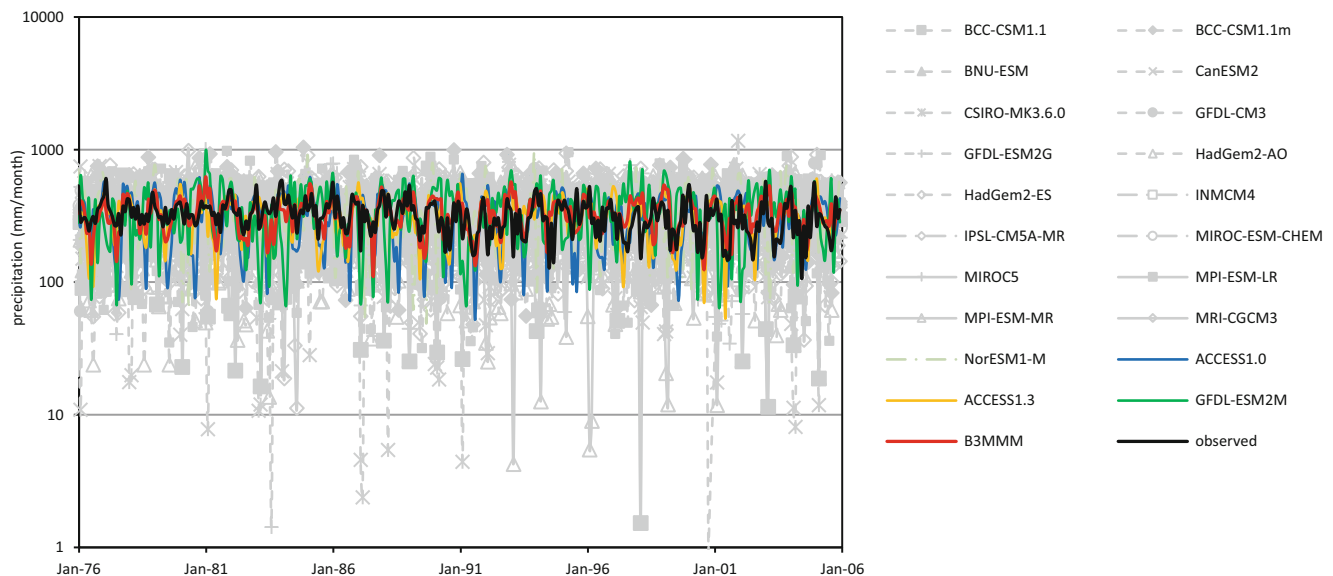
Fig. 3 Monthly precipitation (mm/month) over Grid-A for the period of 1976–2005, comparison of observed monthly precipitation with simulated monthly precipitation by 20 GCMs

GFDL-ESM2M were selected to develop the multi-model mean ensemble of B3MMM. Another recent study by Raghavan et al. (2017) also assessed the 10 GCMs (excluding ACCESS1.0, ACCESS1.3, and GFDL-ESM2M) from CMIP5 for their capability to simulate precipitation over SEA. It is noted that most of the models unable to reproduce the observed climate of the SEA; multi-model mean ensemble of all ten models represented the better results for the observed climate but uncertainties with the individual models are very high. Therefore, whilst using the multi-model mean ensemble for future climate projection, special care should be taken for selection of high-performing models and elimination of the low-performing model. In this study, we screened 20 GCMs for their capability to simulate the observed precipitation over Central Sarawak and adopted mean ensemble (B3MMM) of three highest ranked models for future projection of precipitation over the RRB. The B3MMM also reproduced the observed precipitation more realistically compared to the individual models as shown in Fig. 3.

4.2 Validation of WeaGETS

Using 30-year observed daily precipitation in WeaGETS, 120-year daily precipitation time series were generated at all rainfall stations in the RRB. WeaGETS capability for precipitation generation was assessed using three statistical indicators, i.e. RMSE, NSE and MBE. The model successfully generated the monthly precipitation as the NSE at all stations was greater than 80%, MBE of less than 1%, and RMSE ranging from 104 to 164 mm per month as shown in Table 4.

The mean monthly generated precipitation was compared with observed precipitation to assess the WeaGETS capability to preserve the LFV in the generated precipitation (Fig. 4). The spectral correction approach used for the LFV correction performed well as it reproduced the mean precipitation for all of the months accurately, which also indicate that the model was capable of reproducing the precipitation pattern over the RRB.

Compared to another study in Malaysia by Hassan et al. (2014), our results indicate that the model successfully generated the mean monthly precipitation over the selected rainfall stations as given in Table 4. Hassan et al. (2014) used the SDSM and LARS-WG to generate precipitation over three location in Peninsular Malaysia and found that SDSM overestimated the mean monthly precipitation especially at the stations in the central and southern part of Peninsular Malaysia during the model validation, whilst LAR-WG under-estimated the monthly precipitation in the central station in Peninsular Malaysia. In this study, WeaGETS showed the consistent performance for precipitation generation at all rainfall stations in the upper and lower RRB and therefore, it

Table 4 Performance of WeaGETS for generating precipitation over RRB. 120-year generated monthly precipitation was compared with the observed monthly precipitation (1976–2005) at six rainfall stations

| Station	Monthly rainfall mm	NSE %	MBE %	RMSE mm/month
(a) Nanga Busang				
Observed	344.6			
Generated	343.8	84	0.20	147
(b) Nanga Entawau				
Observed	384.1			
Generated	385.4	84	0.35	164
(c) Long Laku				
Observed	327.5			
Generated	328.3	82	0.24	151
(d) Matu				
Observed	282.0			
Generated	283.1	84	0.40	131
(e) Sibu				
Observed	267.2			
Generated	267.9	81	0.28	126
(f) Song				
Observed	280.5			
Generated	280.6	88	0.04	104

provides sensible projection of annual and seasonal precipitation over the RRB.

We also plotted the double mass curves for daily observed precipitation against the generated precipitation; WeaGETS reproduced the precipitation amount accurately over the 30-year period as shown in Fig. 5. The model slightly under-/over-estimated the precipitation in the middle period at two stations, i.e. Long Laku and Sibu, but overall WeaGETS reproduced the same amount of precipitation over the 30-year period, which provide further confidence on the approach used for the precipitation projected over the RRB as we compared the 30-year period for our assessment.

4.3 Future precipitation projection

4.3.1 Variation in mean annual precipitation

To assess potential impact of the climate change on precipitation, we analysed future projected precipitation for three future periods, i.e. 2020s, 2050s, and 2080s. The mean annual projected precipitation under B3MMM at all of the stations for three future periods was compared with the mean annual observed precipitation (1976–2006) as given in Table 5 and shown in Fig. 6. The kriging (Gaussian process regression) method in Arc GIS tool was used to interpolate and exhibit the point precipitation at all 25 rainfall stations into the basin
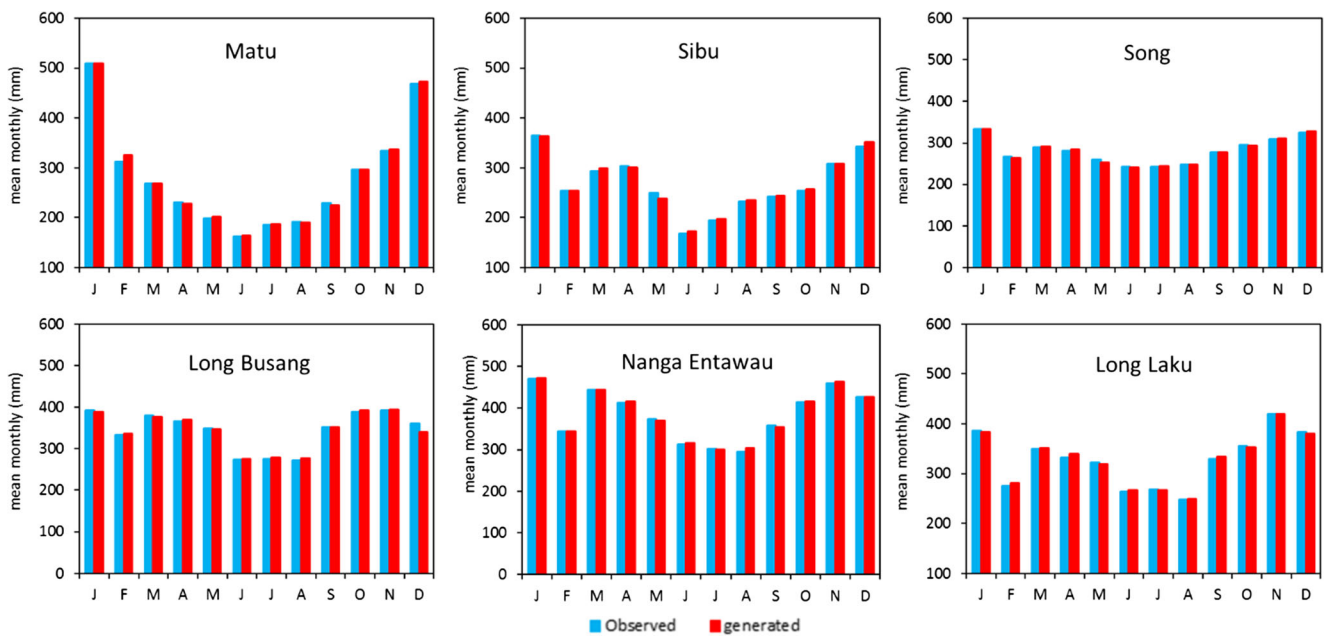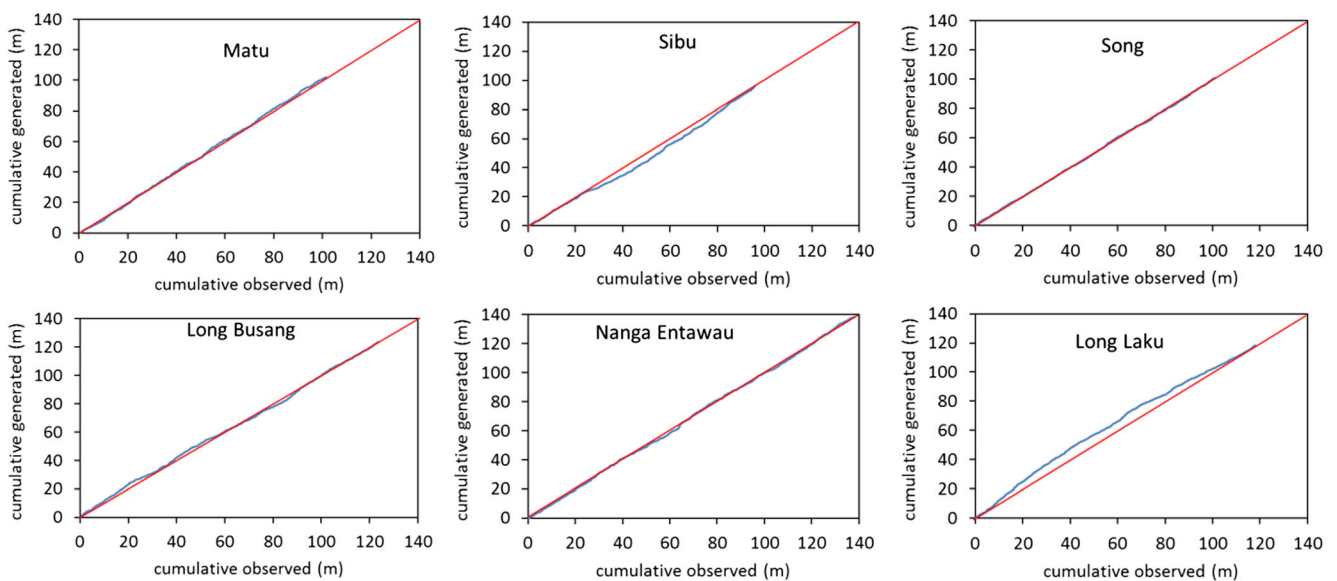
Fig. 4 Comparison of monthly observed precipitation (1976–2005) vs. WeaGETS generated precipitation at six rainfall stations in RRB

precipitation (i.e. Fig. 6). It was projected that the upper RRB would have 3, 3, and 7% increase in precipitation during 2020s, 2050s, and 2080s, respectively, under RCP4.5. Under RCP8.5, upper RRB would have 6, 7, and 12% increase in annual precipitation during the 2020s, 2050s, and 2080s, respectively. For the lower RRB, it is projected to have 1% decrease during 2020s and 4 and 7% increase during 2050s and 2080s under RCP4.5. And under RCP8.5, it is projected to have 4, 5, and 8% increase in annual precipitation during 2020s, 2050s, and 2080s, respectively. Overall, there is an increasing trend in the mean annual precipitation in the future. We applied the trend analysis to assess the significance in the

historical and future annual precipitation and it is discussed in Sect. 4.4.

4.3.2 Intra-annual variability in future precipitation

Seasonal change in precipitation were assessed for the future periods of 2020s, 2050s, and 2080s under both RCPs as shown in Figs. 7, 8, 9, and 10. DJF is the wettest season in RRB as shown in Fig. 2; during DJF, it is projected that the RRB would have higher increase in precipitation under RCP8.5 compared to RCP4.5. But during 2020s, upper RRB is projected to receive higher DJF precipitation under RCP4.5


Fig. 5 Double mass plot for daily observed precipitation (1976–2005) vs. WeaGETS generated precipitation at six rainfall stations in the RRB

Table 5 Percentage (%) changes in mean annual and seasonal precipitation over RRB under RCP4.5 and RCP8.5 of B3MMM, comparison of future periods with the baseline period of 1976–2005

Sub-basin	RCP4.5					RCP8.5				
	Annual	DJF	MAM	JJA	SON	Annual	DJF	MAM	JJA	SON
Upper RRB										
2020s	3	9	0	3	1	6	6	10	7	2
2050s	3	2	8	4	− 1	7	6	9	14	0
2080s	7	1	11	15	2	12	11	18	16	5
Lower RRB										
2020s	− 1	− 3	1	0	− 1	4	3	9	4	− 1
2050s	4	4	6	6	− 2	5	3	8	15	− 2
2080s	7	4	7	16	3	8	8	11	13	0

compared to 2050s and 2080s. Under RCP8.5, it is projected to receive 11 and 8% increase in DJF precipitation in the upper and lower RRB, respectivly. Overall, this season is expecting increase in future precipitation under RCP8.5 as shown in Fig. 7. The

MAM is the period when RRB receives the average precipitation and it is noted that this season is projected to have increase in future precipitation (Fig. 8) under both scenarios during all future periods except RCP4.5 of the 2020s when it is expected to
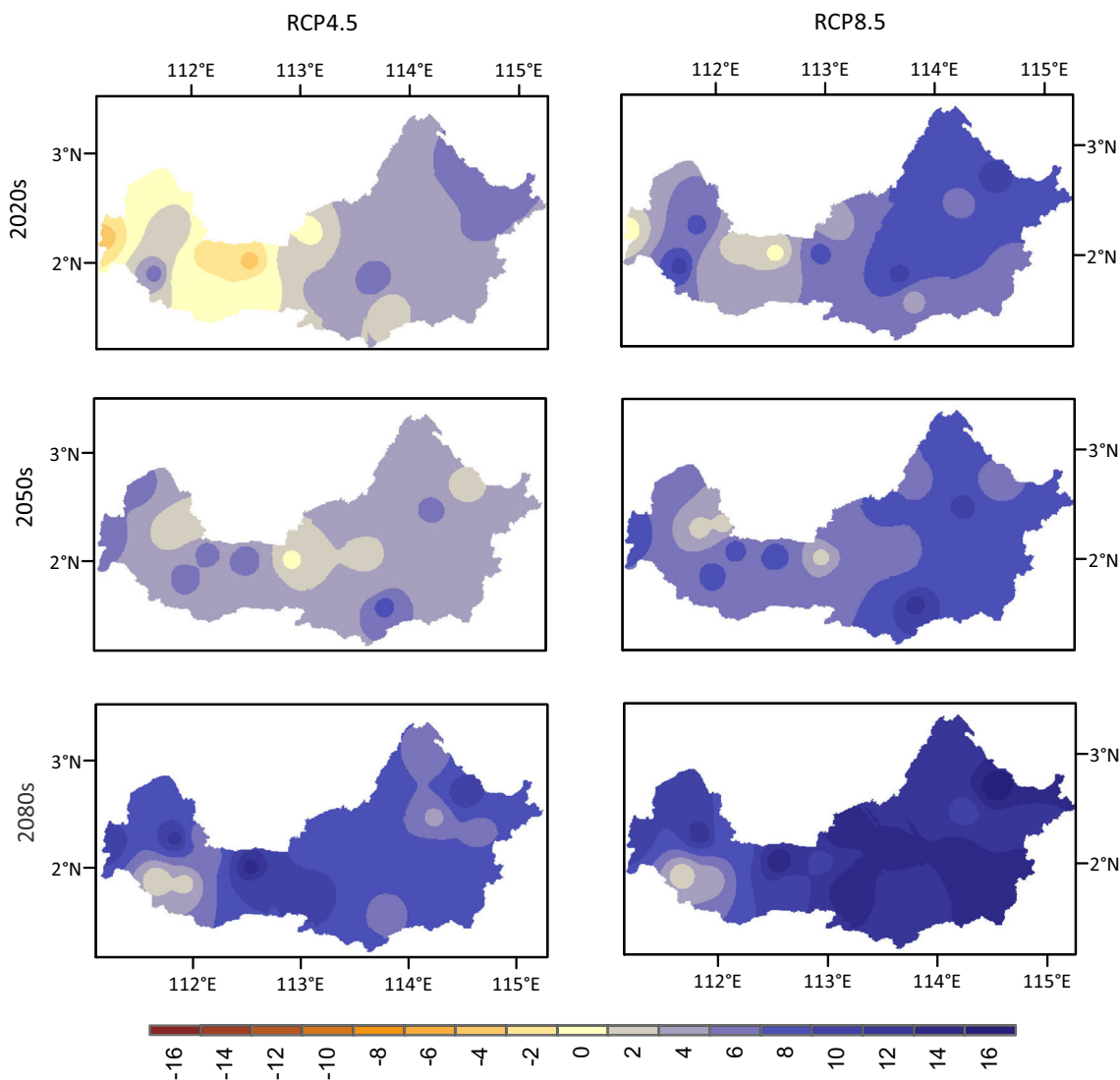
Fig. 6 Percentage (%) changes in the mean annual precipitation over RRB during 2020s, 2050s, and 2080s with respect to baseline period (1976–2005)
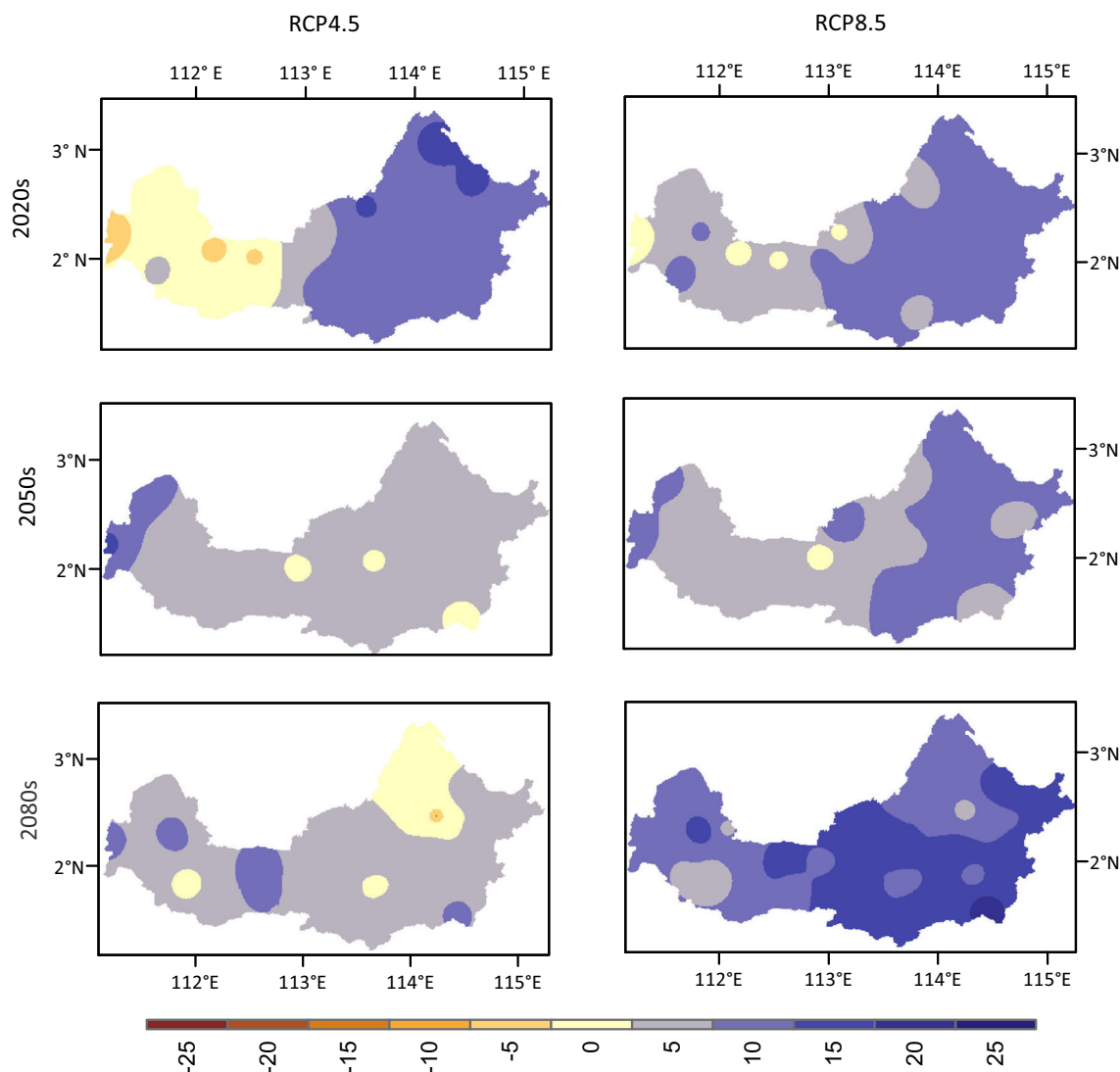
Fig. 7 Percentage (%) changes in DJF precipitation over RRB during 2020s, 2050s, and 2080s with respect to baseline period (1976–2005)

be same as of historical period (as stated in Table 5). During 2080s, it is expected to have 18 and 11% increases in MAM precipitation in the upper and lower RRB, respectively, under RCP8.5, which indicate that this season would be getting wetter in future under RCP8.5.

The JJA is the driest season in the RRB and receives the lowest precipitation over the river basin; it is projected to have increase in precipitation in future under both of the RCPs (Fig. 9). However, during the 2020s, the lower RRB would be stabilised under RCP4.5. During 2080s, the JJA precipitation is projected to increase significantly under RCP8.5, i.e. by 16% increase in the upper RRB and 13% increase in lower RRB. The SON is wetter season in the RRB and this seasonal is projected to be most stable in the future (Fig. 10), whilst it is expected to have up to 5% increase in SON precipitation in the upper RRB during 2080s. We also performed the Mann-

Kendall test to assess the significance on seasonal trend in the precipitation and discussed in Sect. 4.4.

4.3.3 Changes in extreme monthly precipitation

We assessed the change in extreme monthly precipitation over the upper and lower RRB during the future periods under the both RCP4.5 and RCP8.5. It was noted that the extreme monthly precipitation would increase under both scenarios (Fig. 11). Under RCP4.5, the upper RRB would have 29, 43, and 67% increase in extreme monthly precipitation during 2020s, 2050s, and 2080s, respectively. The lower RRB would have 2% decrease and 21 and 58% increase in extreme monthly precipitation during 2020s, 2050s, and 2080s, respectively, as shown in Fig. 11. Under RCP8.5, the results show larger increase in extreme monthly precipitation in upper and lower
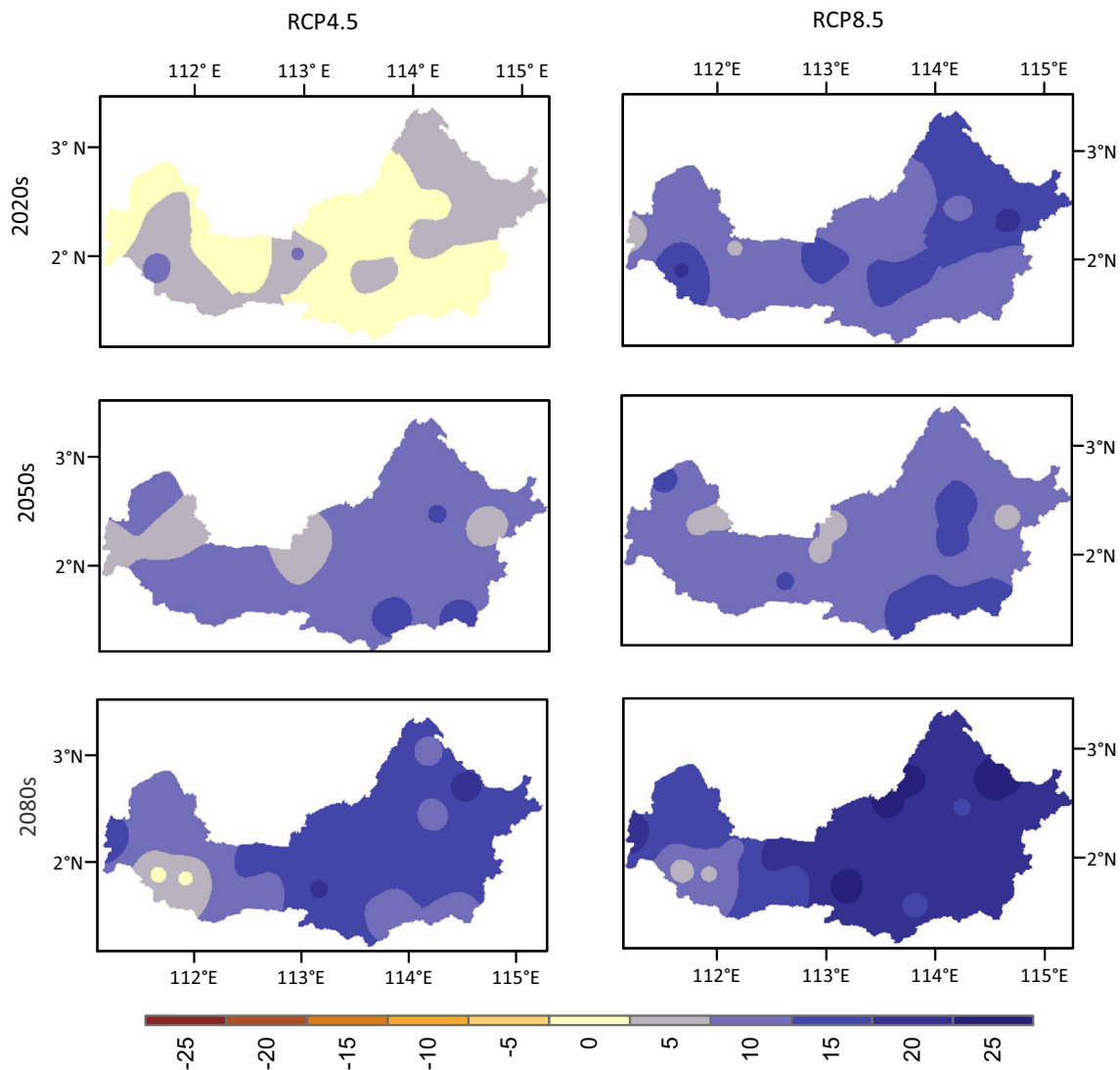
Fig. 8 Percentage (%) changes in MAM precipitation over RRB during 2020s, 2050s, and 2080s with respect to baseline period (1976–2005)

RRB, with 43, 57, and 104% increase in extreme monthly precipitation during 2020s, 2050s, and 2080s, respectively, in the upper RRB and 17, 21, and 51% increase in extreme monthly precipitation during 2020s, 2050s, and 2080s, respectively, in lower RRB. Overall, upper RRB which covers mountainous regions would expect most robust change in extreme monthly precipitation compared to the lower RRB which covers mid land and coastal region.

4.4 Precipitation trend analysis

Mann-Kendall trend test was performed on the annual and seasonal precipitation in upper and lower RRB for the historical period of 1976 to 2005 and future period of 2011 to 2100. For the historical period, the upper RRB has significantly positive trend in the annual precipitation and lower RRB has significantly negative trend in annual precipitation as shown in Table 6. For the seasonal analysis, the upper RRB does not

have the significant trend in the seasonal precipitation except SON, which has significantly positive trend during the historical period. On other hand, the historical precipitation in the lower RRB has significant negative trend during all of the seasons.

For the future period of 2011 to 2100, the annual precipitation has significant positive trend over the RRB under both of the RCPs; it is demonstrated in Fig. 6 as well, where the mean annual precipitation is projected to increase significantly in the future. On seasonal scale, the DJF precipitation has significant negative trend in the upper RRB under RCP4.5 whilst significant positive trend under RCP8.5. The negative trend under the RCP4.5 is understandable as this season projected to higher increase in precipitation during 2020s compared to the 2050s and 2080s of RCP4.5. The lower RRB has significant positive trend during DJF under both of the RCPs. In MAM, the upper RRB has significant positive trend in the future under both RCPs and in the lower RRB,
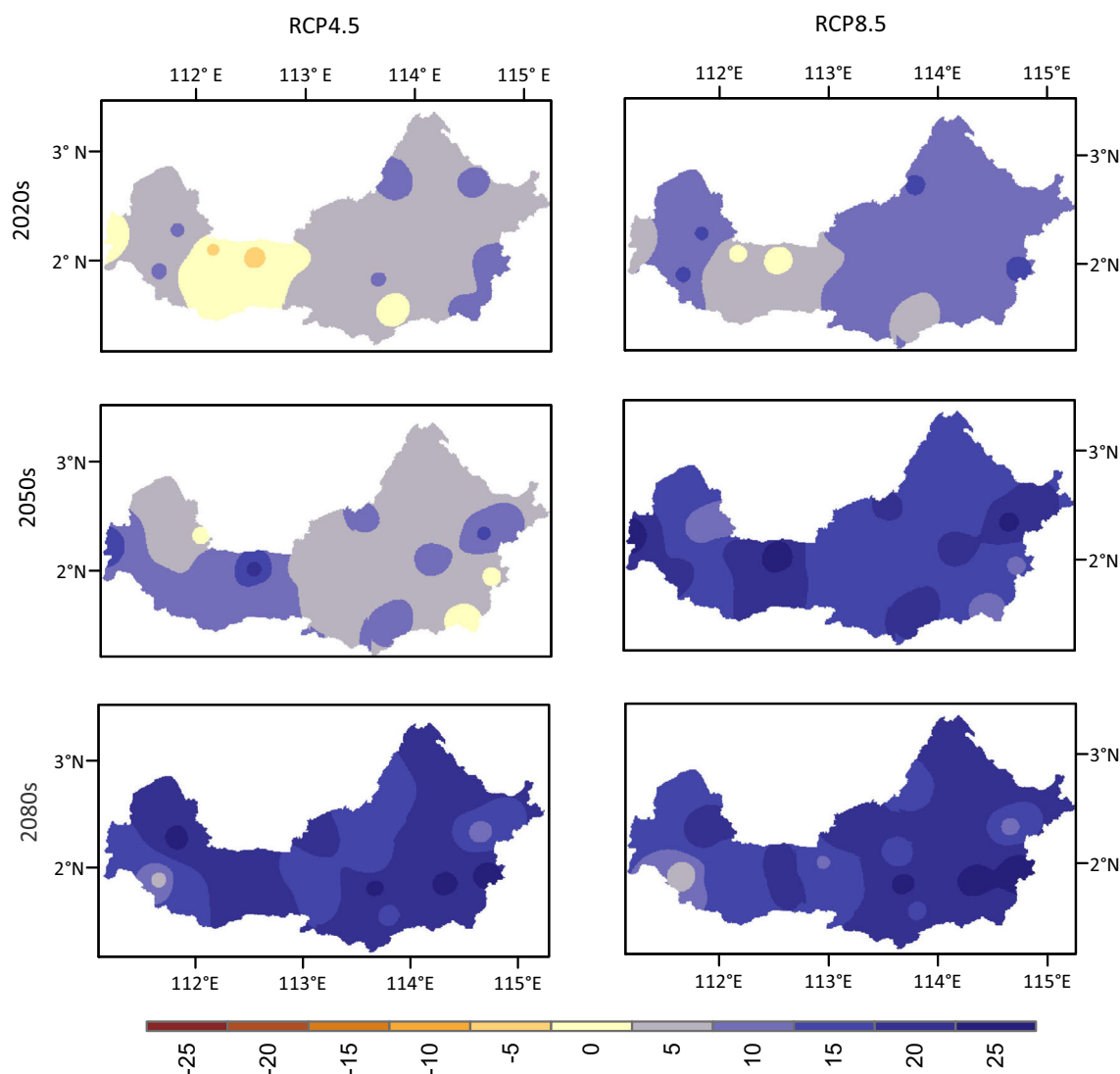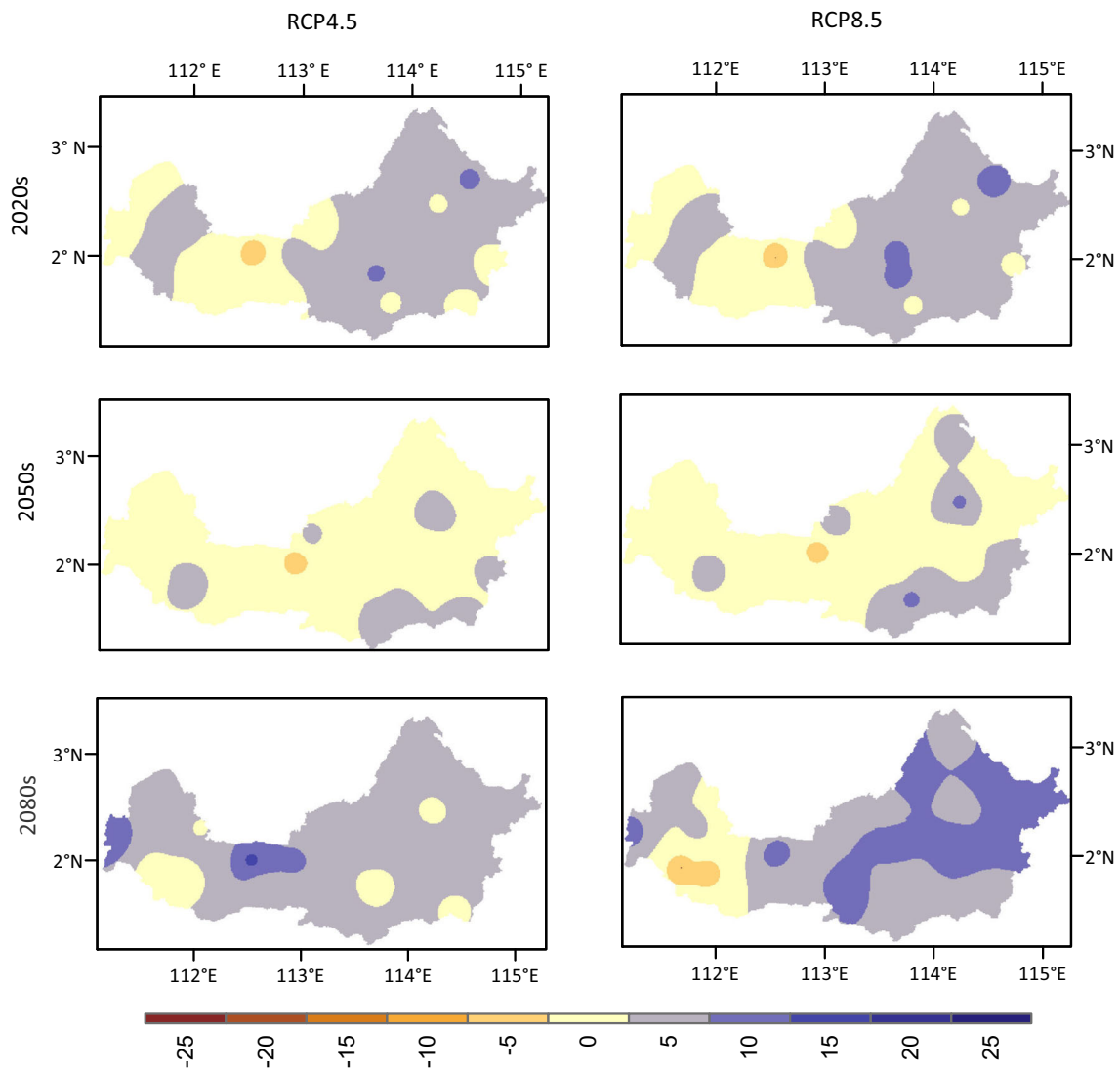
Fig. 9 Percentage (%) changes in JJA precipitation over RRB during 2020s, 2050s, and 2080s with respect to baseline period (1976–2005)

significant positive trend under RCP4.5, and positive but insignificant under RCP8.5. The JJA precipitation has significant positive trend in the whole RRB (Table 6) and it can be seen in Fig. 9, where the precipitation is projected to increase significantly in the three future periods. As the SON precipitation is projected to be little changed in future (up to 5%), the trend analysis also asserts that there is no significant trend in future precipitation during this season, except in lower RRB, where it has significant positive trend under RCP4.5. Overall, the RRB would be expecting significant increase in future precipitation under both of the RCPs.

4.5 Further discussion

Projection of variability in precipitation over the RRB indicates that there will be increase in annual precipitation under both future climate scenarios. However, RCP8.5 shows larger

increase in annual precipitation compared to RCP4.5. The similar projection exhibited by MetMalaysia (2009), which compared the period of (2001–2099) with baseline period of (1991–1999) over the whole Malaysia. Amin et al. (2016) also projected the future precipitation on several river basins in Sabah and Sarawak and noted increase in precipitation over RRB under the future climate when compared with the present day climate. The results of this study were also supported by the conclusion of several recent studied conducted by (Hsu et al. 2012; Kitoh et al. 2013; Lee and Wang 2012; Wang et al. 2013), which exhibit notable increase in global monsoon precipitation due to changing climate during the twenty-first century. Kitoh et al. (2013) compared future projections of global monsoon under RCP4.5 and RCP8.5 scenarios and noted that under RCP8.5, global monsoon has larger and more robust response to atmospheric warming. Taylor et al. (2012) also assessed the

Fig. 10 Percentage (%) changes in SON precipitation over RRB during 2020s, 2050s, and 2080s with respect to baseline period (1976–2005)
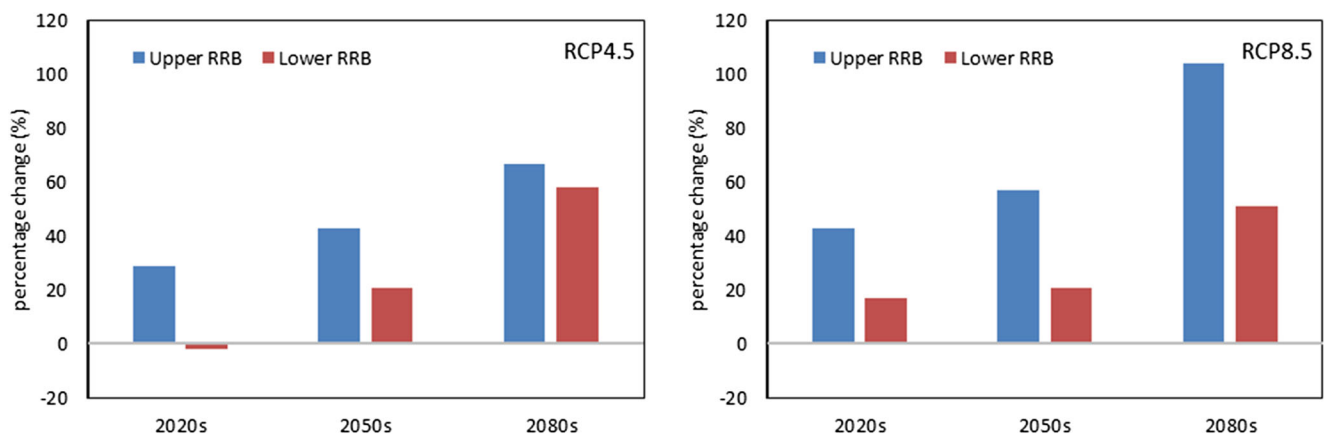
Fig. 11 Percentage (%) changes in extreme monthly precipitation over RRB; comparison of extreme monthly precipitation under future climate (2020s, 2050s, and 2080s) with the baseline period of 1976–2005

Table 6 Mann-Kendall's non-parametric trend test: Kendall's τ computed for annual and seasonal precipitation at upper and lower RRB. ** indicate the p value < 0.01 and * indicate the p value < 0.05

Sub-basin	Historical 1976–2005		RCP4.5 2011–2100		RCP8.5 2011–2100	
	τ	p	τ	p	τ	p
Annual						
Upper RRB	0.40	**	0.17	*	0.25	**
Lower RRB	− 0.55	**	0.36	**	0.19	**
DJF						
Upper RRB	0.16		−0.24	**	0.21	**
Lower RRB	− 0.30	*	0.21	**	0.18	*
MAM						
Upper RRB	0.17		0.36	**	0.20	**
Lower RRB	− 0.47	**	0.18	*	0.06	
JJA						
Upper RRB	0.18		0.22	**	0.16	*
Lower RRB	− 0.48	**	0.39	**	0.24	**
SON						
Upper RRB	0.34	*	0.04		0.12	
Lower RRB	− 0.39	**	0.18	*	0.08	

CMIP5 models under RCPs and noted that the extreme precipitation event will be more frequent in the tropical regions by the end of this century.

Under present day climate of SEA, the northeast monsoon starts in October and continues until March and southwest monsoon starts from late May and continue until September. However, the RRB receives heavy precipitation even during the intermonsoon period of April and May. Under projected future climate, it was expected that the RRB would receive more precipitation during MAM. There is limited literature on how this synoptic phenomenon relate to local climate and there is a need to study the intermonsoon physical phenomenon in this region. During JJA, RRB is expected to have more southwest moonsoon rainfalls over the catchment under the future periods; however, under the present day climate, this season receives the lowest monthly precipitation over the RRB. It will benefit the hydropower reservoirs in the river basin as it will provide the water security to the reservoirs during these lowest inflow months. The upper RRB lies in the high mountainous region and lower RRB covers midland and coastal areas; most of the inhabitants settled in the lower RRB and are vulnerable to the potential flood risk in future. Therefore, potential increase in maximum monthly precipitation caution the water resource planners to workout insightful action plan on the flood risk management and early warning system for the RRB.

5 Conclusions

During the evaluation of twenty GCMs over the RRB, ACCESS1.0, ACCESS1.3, and GFDL-ESM2M were the most suitable GCMs to be used for the future precipitation projection over the RRB. This study also concludes that the annual precipitation over the RRB expected to increase over the river basin under RCP4.5 and RCP8.5. Similar trend is projected for the seasonal precipitation, especially during the MAM, when the increase in precipitation is more robust for both scenarios. Borneo is the largest island in Asia and it has some of the largest river basins in the region such as Kapuas River Basin in West Kalimantan, Barito River Basin in South Kalimantan, Kayan River Basin in North Kalimantan, and RRB in Sarawak. This study will be useful to assess the climate resilience in these major river basins of Borneo. However, to illuminate the capability to simulate precipitation over these river basins, there is also a need to extend GCMs evaluation on a larger area, i.e. over the whole Borneo.

References

Amin MZM, Shaaban AJ, Ohara N, Kavvas ML, Chen ZQ, Kure S, Jang S (2016) Climate change assessment of water resources in Sabah and Sarawak, Malaysia, based on dynamically-downscaled GCM projections using a regional hydroclimate model. J Hydrol Eng 21: 05015015. https://doi.org/10.1061/(ASCE)HE.1943-5584.0001242

Buishand TA (1978) Some remarks on the use of daily rainfall models. J Hydrol 36:295–308

Campozano L, Tenelanda D, Sanchez E, Samaniego E, Feyen J (2016) Comparison of statistical downscaling methods for monthly total precipitation: case study for the Paute River Basin in southern Ecuador. Adv Meteorol 2016:1–13. https://doi.org/10.1155/2016/6526341

Chattopadhyay S, Edwards D (2016) Long-term trend analysis of precipitation and air temperature for Kentucky, United States. Climate 4: 10. https://doi.org/10.3390/cli4010010

Chen J, Brissette FP (2014) Comparison of five stochastic weather generators in simulating daily precipitation and temperature for the

Loess Plateau of China. Int J Climatol 34:3089–3105. https://doi.org/10.1002/joc.3896

Chen J, Zhang X-c, Liu W-z, Li Z (2009) Evaluating and extending CLIGEN precipitation generation for the Loess Plateau of China. J Am Water Resour Assoc 45:378–396. https://doi.org/10.1111/j.1752-1688.2008.00296.x

Chen J, Brissette FP, Leconte R (2010) A daily stochastic weather generator for preserving low-frequency of climate variability. J Hydrol 388:480–490. https://doi.org/10.1016/j.jhydrol.2010.05.032

Chiew FHS, Teng J, Vaze J, Post DA, Perraud JM, Kirono DGC, Viney NR (2009) Estimating climate change impact on runoff across southeast Australia: method, results, and implications of the modeling method. Water Resour Res 45:W10414. https://doi.org/10.1029/2008wr007338

Chu JT, Xia J, CY X, Singh VP (2010) Statistical downscaling of daily mean temperature, pan evaporation and precipitation for climate change scenarios in Haihe River, China. Theor Appl Climatol 99:149–161

Collins M (2007) Ensembles and probabilities: a new era in the prediction of climate change. Philos Trans Ser A Math Phys Eng Sci 365:1957–1970. https://doi.org/10.1098/rsta.2007.2068

Doty B (1995) The grid analysis and display system. User manual

Feng G, Cobb S, Abdo Z, Fisher DK, Ouyang Y, Adeli A, Jenkins JN (2016) Trend analysis and forecast of precipitation, reference evapotranspiration, and rainfall deficit in the Blackland Prairie of eastern Mississippi. J Appl Meteorol Climatol 55:1425–1439. https://doi.org/10.1175/jamc-d-15-0265.1

Forsythe N et al (2014) Application of a stochastic weather generator to assess climate change impacts in a semi-arid climate: the Upper Indus Basin. J Hydrol 517:1019–1034. https://doi.org/10.1016/j.jhydrol.2014.06.031

Fowler HJ, Ekström M (2009) Multi-model ensemble estimates of climate change impacts on UK seasonal precipitation extremes. Int J Climatol 29:385–416. https://doi.org/10.1002/joc.1827

Gilbert RO (1987) Statistical methods for environmental pollution monitoring. Wiley, New York

Gregory JM, Wigley TML, Jones PD (1993) Application of Markov models to area-average daily precipitation series and interannual variability in seasonal totals. Clim Dyn 8:299–310

Groisman PY, Knight RW, Easterling DR, Karl TR (2005) Trends in intense precipitation in the climate record. J Climate 18:1326–1350. https://doi.org/10.1175/jcli3339.1

Hansen JW, Mavromatis T (2001) Correcting low-frequency variability bias in stochastic weather generators. Agric For Meteorol 109:297–310

Hanson CL, Cumming KA, Woolhiser DA, Richardson CW (1994) Microcomputer program for daily weather simulations in the contiguous United States. USDA-ARS Publ ARS-114, Washington, DC

Hasan D.S.N.A.PA., Ratnayake U, Shams S, Nayan ZBH, Rahman EKA (2017) Prediction of climate change in Brunei Darussalam using statistical downscaling model. Theor Appl Climatol. https://doi.org/10.1007/s00704-017-2172-z

Hassan Z, Shamsudin S, Harun S (2014) Application of SDSM and LARS-WG for simulating and downscaling of rainfall and temperature. Theor Appl Climatol 116:243–257

Hassan M, Du P, Jia S, Iqbal W, Mahmood R, Ba W (2015) An assessment of the South Asian summer monsoon variability for present and future climatologies using a high resolution regional climate model (RegCM4.3) under the AR5 scenarios. Atmosphere 6:1833–1857. https://doi.org/10.3390/atmos6111833

Hasson S, Pascale S, Lucarini V, Böhner J (2016) Seasonal cycle of precipitation over major river basins in South and Southeast Asia: a review of the CMIP5 climate models data for present climate and future climate projections. Atmos Res 180:42–63. https://doi.org/10.1016/j.atmosres.2016.05.008

Hirsch RM, Slack JR, Smith RA (1982) Techniques of trend analysis for monthly water quality data. Water Resour Res 18:107–121. https://doi.org/10.1029/WR018i001p00107

Hsu P, Li T, Luo JJ, Murakami H, Kitoh A, Zhao M (2012) Increase of global monsoon area and precipitation under global warming: a robust signal? Geophys Res Lett 39:L06701. https://doi.org/10.1029/2012gl051037

Hussain M, Nadya S, Yusof KW, Mustafa MR (2017a) Potential impact of climate change on inflows to the Batang Ai reservoir, Malaysia. Int J Hydropower Dams 24:44–48

Hussain M, Yusof KW, Mustafa MR, Mahmood R, Shaofeng J (2017b) Projected changes in temperature and precipitation in Sarawak state of Malaysia for selected CMIP5 climate scenarios. Int J Sustain Dev Plan 12:1299–1311. https://doi.org/10.2495/sdp-v12-n8-1299-1311

IPCC (2013) Summary for policymakers. In: Stocker TF et al (eds) Climate Change 2013: the physical science basis. Contribution of Working Group I to the Fifth Assessment Report of the Intergovernmental Panel on Climate Change. Cambridge University Press, Cambridge 17 pp

Islam MA, Chowdhury RI (2006) A higher order Markov model for analyzing covariate dependence. Appl Math Model 30:477–488. https://doi.org/10.1016/j.apm.2005.05.006

Johnson GL, Hanson CL, Hardegree SP, Ballard EB (1996) Stochastic weather simulation: overview and analysis of two commonly used models. J Appl Meteorol 35:1878–1896

Jones PD, Harpham C, Goodess CM, Kilsby CG (2011) Perturbing a weather generator using change factors derived from regional climate model simulations. Nonlinear Proc Geophys 18:503–511. https://doi.org/10.5194/npg-18-503-2011

Juneng L et al (2016) Sensitivity of southeast Asia rainfall simulations to cumulus and air-sea flux parameterizations in RegCM4. Clim Res 69:59–77. https://doi.org/10.3354/cr01386

Katz RW, Parlange MB (1993) Effects of an index of atmospheric circulation on stochastic properties of precipitation. Water Resour Res 29:2335–2344

Kendall MG (1975) Rank Correlation Methods, 4th edn. Charles Griffin, London

Kilsby CG et al (2007) A daily weather generator for use in climate change studies. Environ Model Softw 22:1705–1719. https://doi.org/10.1016/j.envsoft.2007.02.005

Kitoh A, Endo H, Krishna Kumar K, Cavalcanti IFA, Goswami P, Zhou T (2013) Monsoons in a changing world: a regional perspective in a global context. J Geophys Res-Atmos 118:3053–3065. https://doi.org/10.1002/jgrd.50258

Knutti R, Furrer R, Tebaldi C, Cermak J, Meehl GA (2010) Challenges in combining projections from multiple climate models. J Clim 23:2739–2758. https://doi.org/10.1175/2009jcli3361.1

Kum D et al (2014) Projecting future climate change scenarios using three bias-correction methods. Adv Meteorol 2014:1–12. https://doi.org/10.1155/2014/704151

Kumagai T et al (2004) Water cycling in a Bornean tropical rain forest under current and projected precipitation scenarios. Water Resour Res 40:W01104. https://doi.org/10.1029/2003wr002226

Lee J-Y, Wang B (2012) Future change of global monsoon in the CMIP5. Clim Dynam 42:101–119. https://doi.org/10.1007/s00382-012-1564-0

Loh JL, Tangang F, Juneng L, Hein D, Lee D-I (2016) Projected rainfall and temperature changes over Malaysia at the end of the 21st century based on PRECIS modelling system. Asia-Pac J Atmos Sci 52:191–208. https://doi.org/10.1007/s13143-016-0019-7

Mahmood R, Babel MS (2012) Evaluation of SDSM developed by annual and monthly sub-models for downscaling temperature and precipitation in the Jhelum basin, Pakistan and India. Theor Appl Climatol 113:27–44. https://doi.org/10.1007/s00704-012-0765-0

Mann HB (1945) Non-parametric tests against trend. Econometrica 13:163–171

McSweeney CF et al. (2015) Singapore's second national climate change study—climate projections to 2100—chapter 3

MetMalaysia (2009) Climate change scenarios for Malaysia 2001–2099

Nash JE, Sutcliffe JV (1970) River flow forecasting through conceptual models part I—a discussion of principles. J Hydrol 10:282–290. https://doi.org/10.1016/0022-1694(70)90255-6

Nicks AD, Lane LJ, Gander GA (1995) Weather Generator. In: Flanagan, DC, Nearing, MA (Eds), USDA-Water Erosion Prediction Project: hillslope profile and watershed model documentation, NSERL Report No 10 West Lafayette, Ind: USDA-ARS-NSERL (Chapter 2)

Ntegeka V, Baguis P, Roulin E, Willems P (2014) Developing tailored climate change scenarios for hydrological impact assessments. J Hydrol 508:307–321. https://doi.org/10.1016/j.jhydrol.2013.11.001

Olsson J, Berggren K, Olofsson M, Viklander M (2009) Applying climate model precipitation scenarios for urban hydrological assessment: a case study in Kalmar City, Sweden. Atmos Res 92:364–375. https://doi.org/10.1016/j.atmosres.2009.01.015

Raghavan SV, Liu J, Nguyen NS, Vu MT, Liong S-Y (2017) Assessment of CMIP5 historical simulations of rainfall over Southeast Asia. Theor Appl Climatol. https://doi.org/10.1007/s00704-017-2111-z

Raitzer DA, Bosello F, Tavoni M, Orecchia C, Marangoni G, Samson JNG (2015) Southeast asia and the economics of global climate stabilization. Asian Development Bank

Richardson CW (1981) Stochastic simulation of daily precipitation, temperature, and solar radiation. Water Resour Res 17:182–190

Richardson CW, Wright DA (1984) WGEN: A model for generating daily weather variables. US Dept Agric Agriculture Research Service Publ ARS-8

Sarthi PP, Ghosh S, Kumar P (2015) Possible future projection of Indian Summer Monsoon Rainfall (ISMR) with the evaluation of model performance in Coupled Model Inter-comparison Project Phase 5 (CMIP5). Glob Planet Chang 129:92–106. https://doi.org/10.1016/j.gloplacha.2015.03.005

Semenov MA, Barrow EM (1997) Use of a stochastic weather generator in the development of climate change scenarios. Clim Chang 35:397–414

Semenov MA, Barrow EM (2002) A stochastic weather generator for use in climate impact studies. User manual

Semenov V, Bengtsson L (2002) Secular trends in daily precipitation characteristics: greenhouse gas simulation with a coupled AOGCM. Clim Dynam 19:123–140. https://doi.org/10.1007/s00382-001-0218-4

Semenov MA, Brooks RJ, Barrow EM, Richardson CW (1998) Comparison of the WGEN and LARS-WG stochastic weather generators for diverse climates. Clim Res 10:95–107

Sharmila S, Joseph S, Sahai AK, Abhilash S, Chattopadhyay R (2015) Future projection of Indian summer monsoon variability under climate change scenario: an assessment from CMIP5 climate models. Glob Planet Chang 124:62–78. https://doi.org/10.1016/j.gloplacha.2014.11.004

Siew JH, Tangang FT, Juneng L (2013) Evaluation of CMIP5 coupled atmosphere-ocean general circulation models and projection of the Southeast Asian winter monsoon in the 21st century. Int J Climatol. https://doi.org/10.1002/joc.3880

Sperber KR et al (2012) The Asian summer monsoon: an intercomparison of CMIP5 vs. CMIP3 simulations of the late 20th century. Clim Dyn 41:2711–2744. https://doi.org/10.1007/s00382-012-1607-6

Stephenson DB, Rupa KK, Doblas-Reyes FJ, Royer J-F, Chauvin F (1999) Extreme daily rainfall events and their impact on ensemble forecasts of the Indian Monsoon. Mon Weather Rev 127:1954–1966

Stockle CO, Campbell GS, Nelson R (1999) ClimGen manual. Biological Systems Engineering Department, Washington State University, Pullman

Tan M, Ibrahim A, Duan Z, Cracknell A, Chaplot V (2015) Evaluation of six high-resolution satellite and ground-based precipitation products over Malaysia. Remote Sens 7:1504–1528. https://doi.org/10.3390/rs70201504

Taylor KE (2001) Summarizing multiple aspects of model performance in a single diagram. J Geophys Res 106:7183–7192

Taylor KE, Stouffer RJ, Meehl GA (2012) An overview of CMIP5 and the experiment design. Bull Am Meteorol Soc 93:485–498. https://doi.org/10.1175/bams-d-11-00094.1

Teutschbein C, Seibert J (2010) Regional climate models for hydrological impact studies at the catchment scale:a review of recent modeling strategies. Geography Compass 4(7):834–860. https://doi:10.1111/j.1749-8198.2010.00357.x

Timbal B (2004) Southwest Australia past and future rainfall trends. Clim Res 26:233–249

Veldkamp TIE, Wada Y, Aerts JCJH, Ward PJ (2016) Towards a global water scarcity risk assessment framework: incorporation of probability distributions and hydro-climatic variability. Environ Res Lett 11:024006. https://doi.org/10.1088/1748-9326/11/2/024006

Venkataraman K, Tummuri S, Medina A, Perry J (2016) 21st century drought outlook for major climate divisions of Texas based on CMIP5 multimodel ensemble: implications for water resource management. J Hydrol 534:300–316. https://doi.org/10.1016/j.jhydrol.2016.01.001

Wang B, Yim S-Y, Lee J-Y, Liu J, Ha K-J (2013) Future change of Asian-Australian monsoon under RCP 4.5 anthropogenic warming scenario. Clim Dynam 42:83–100. https://doi.org/10.1007/s00382-013-1769-x

Watterson I, Dix M (2003) Simulated changes due to global warming in daily precipitation means and extremes and their interpretation using the gamma distribution. J Geophys Res-Atmos 108:4379

Wilby RL, Wigley TML (2002) Future changes in the distribution of daily precipitation totals across North America. Geophys Res Lett 9:391-394. https://doi.org/10.1029/2001gl013048

Wilks DS (1989) Conditioning stochastic daily precipitation models on total monthly precipitation. Water Resour Res 25:1429–1439

Wilks DS (1999) Interannual variability and extreme-value characteristics of several stochastic daily precipitation models. Agri Forest Meteorol 93:153–169

Wilks DS (2010) Use of stochastic weather generators for precipitation downscaling. Wiley Interdiscip Rev Clim Chang 1:898–907. https://doi.org/10.1002/wcc.85

Zhang XC, Garbrecht JD (2003) Evaluation of CLIGEN precipitation parameters and their implication on WEPP runoff and erosion prediction. Trans ASAE 46:311–320